Electronic Supplementary Material (ESI) for Materials Chemistry Frontiers.

Supporting Information

Achieving high color purity in multi-resonance thermally activated delayed fluorescence emitters through the substitution-driven design strategy

Wanlin Cai,[a] Cheng Zhong[b] and De-Yin Wu*[a]

[a] *State Key Laboratory of Physical Chemistry of Solid Surface, Collaborative Innovation Center of Chemistry for Energy Materials, and Department of Chemistry, College of Chemistry and Chemical Engineering, Xiamen University, Xiamen, 361005, P. R. China*

[b] *Hubei Key Lab on Organic and Polymeric Optoelectronic Materials, Department of Chemistry, Wuhan University, Wuhan, Hubei 430072, P. R. China*

E-mail: dywu@xmu.edu.cn

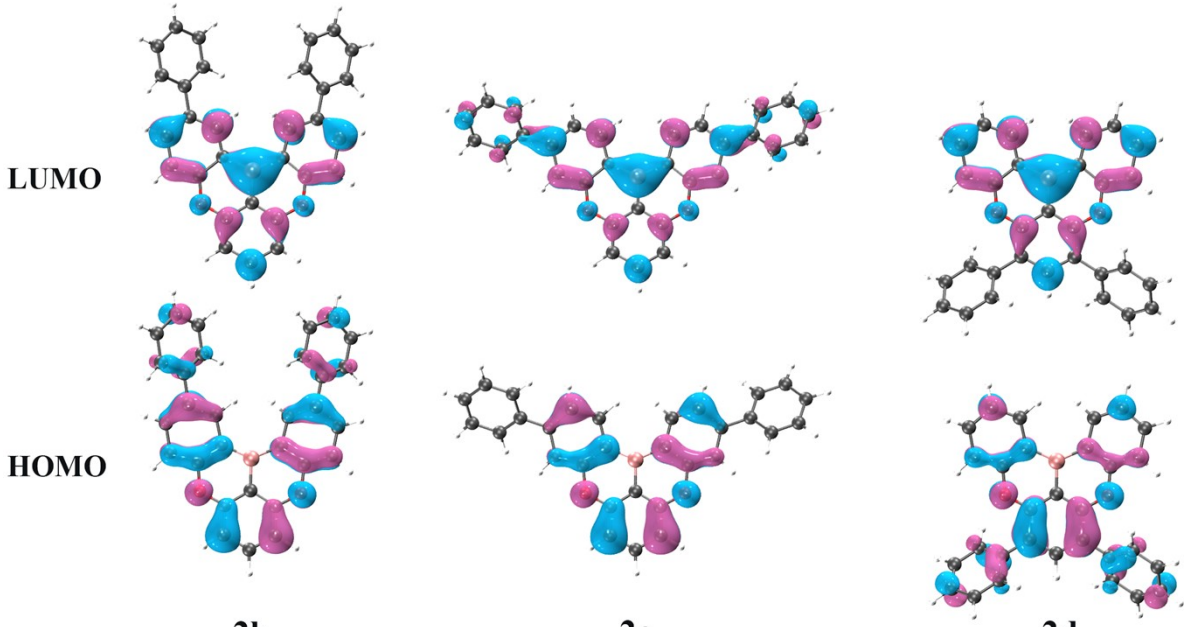

Figure S1. HOMO and LUMO distribution of **2b**, **2c** and **2d**.

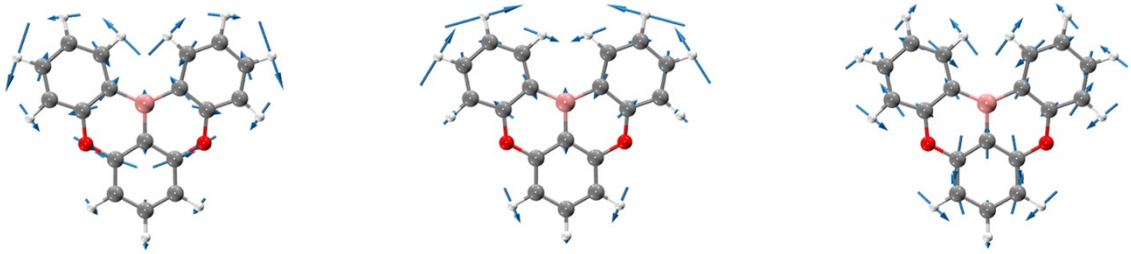

$\omega = 1378.7\ cm^{-1}$
$\lambda = 135.6\ cm^{-1}$

$\omega = 1510.5\ cm^{-1}$
$\lambda = 49.2\ cm^{-1}$

$\omega = 1682.7\ cm^{-1}$
$\lambda = 197.9\ cm^{-1}$

Figure S2. The displacement vectors of the vibration normal modes mainly involved in the low energy region of emission spectrum of **2a**.

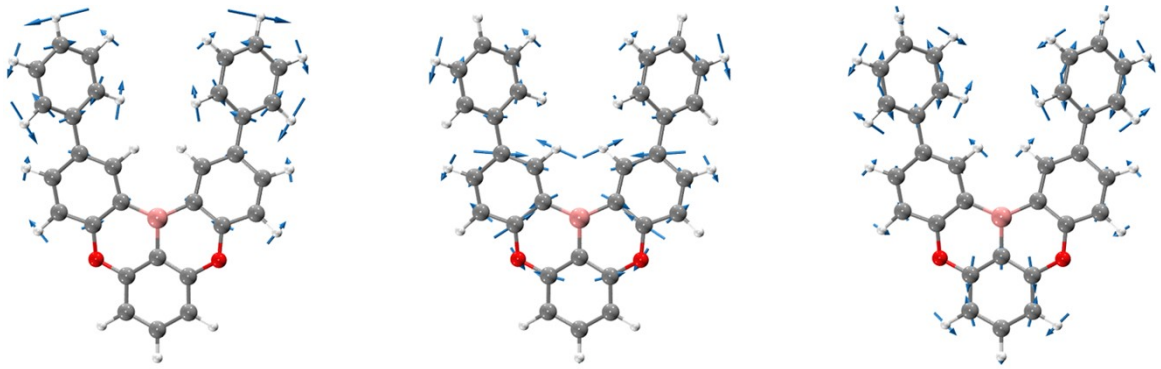

$\omega = 1390.6\ cm^{-1}$
$\lambda = 34.9\ cm^{-1}$

$\omega = 1403.4\ cm^{-1}$
$\lambda = 87.3\ cm^{-1}$

$\omega = 1688.8\ cm^{-1}$
$\lambda = 26.7\ cm^{-1}$

Figure S3. The displacement vectors of the vibration normal modes mainly involved in the low energy region of emission spectrum of **2b**.

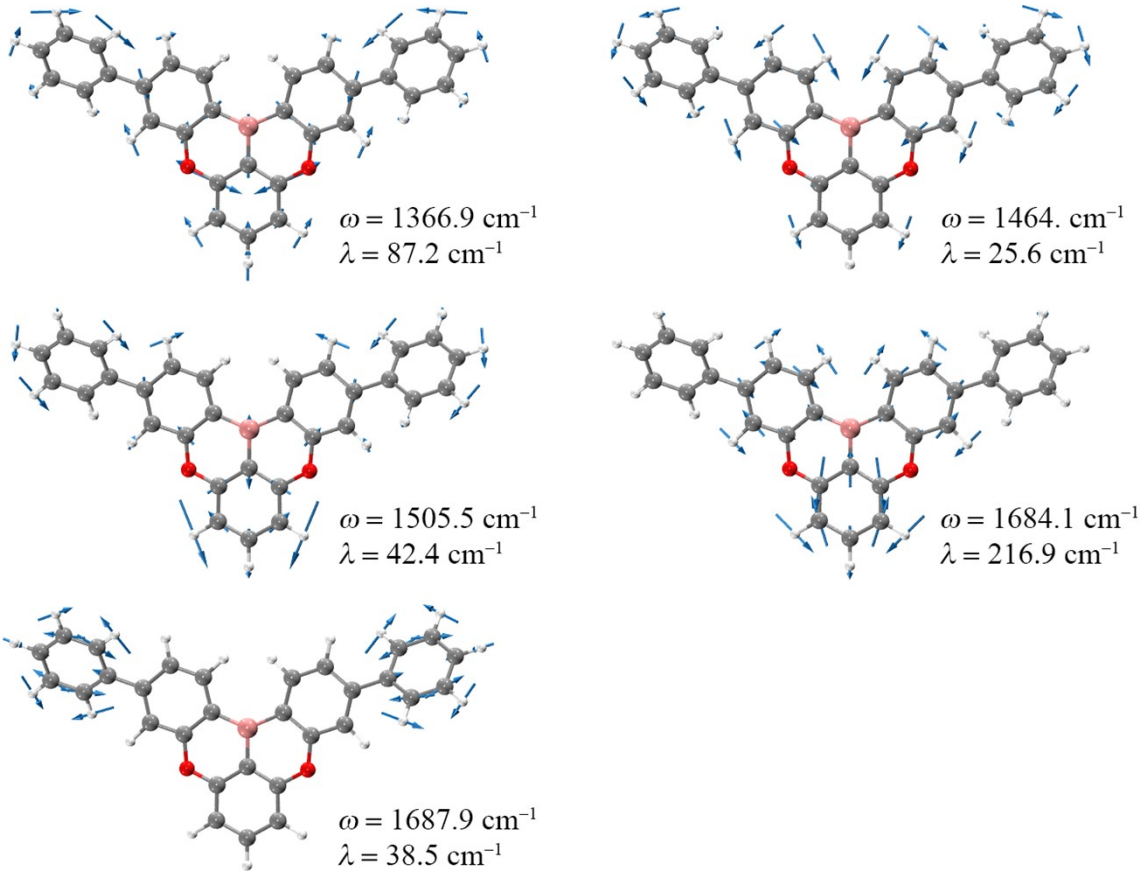

Figure S4. The displacement vectors of the vibration normal modes mainly involved in the low energy region of emission spectrum of **2c**.

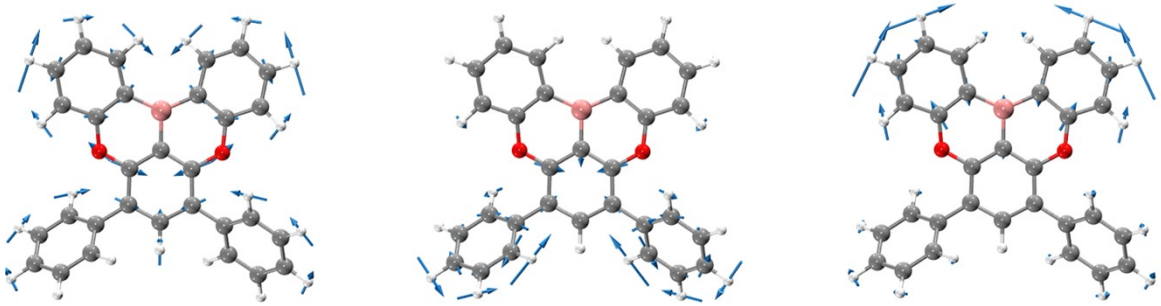

$\omega = 1372.6\ cm^{-1}$
$\lambda = 169.9\ cm^{-1}$

$\omega = 1388.9\ cm^{-1}$
$\lambda = 26.3\ cm^{-1}$

$\omega = 1506.0\ cm^{-1}$
$\lambda = 67.5\ cm^{-1}$

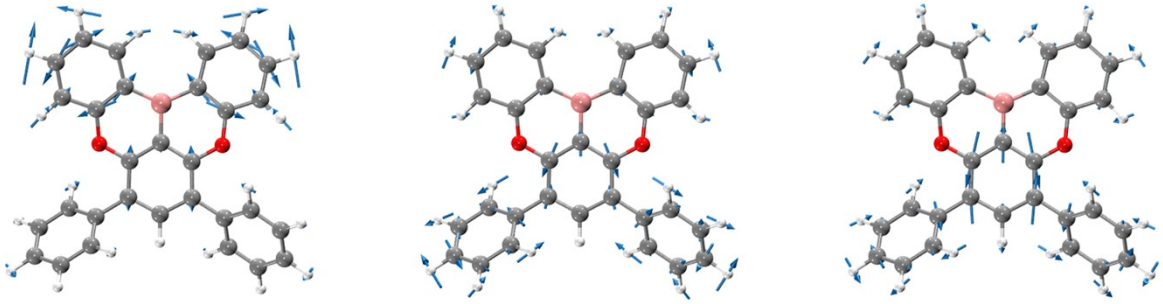

$\omega = 1640.3\ cm^{-1}$
$\lambda = 32.1\ cm^{-1}$

$\omega = 1654.1\ cm^{-1}$
$\lambda = 89.2\ cm^{-1}$

$\omega = 1668.8\ cm^{-1}$
$\lambda = 210.5\ cm^{-1}$

Figure S5. The displacement vectors of the vibration normal modes mainly involved in the low energy region of emission spectrum of **2d**.

Table S1. Calculated bond lengths (Å) at S_0 and S_1 states for **2a** and **2b**.

2a	S_0	S_1	**2b**	S_0	S_1
C1–C2	1.394	1.419	C1–C2	1.394	1.406
C1–C6	1.405	1.392	C1–C6	1.405	1.396
C1–O13	1.349	1.335	C1–O13	1.351	1.349
C2–C3	1.394	1.395	C2–C3	1.395	1.397
C3–C4	1.394	1.395	C3–C4	1.395	1.397
C4–C5	1.394	1.419	C4–C5	1.394	1.406
C5–C6	1.405	1.392	C5–C6	1.405	1.396
C5–O7	1.349	1.335	C5–O7	1.351	1.349
C6–B10	1.522	1.536	C6–B10	1.519	1.526
O7–C8	1.358	1.373	O7–C8	1.357	1.358
C8–C9	1.413	1.428	C8–C9	1.411	1.428
C8–C14	1.401	1.392	C8–C14	1.401	1.397
C9–B10	1.551	1.540	C9–B10	1.548	1.541
C9–C17	1.413	1.415	C9–C17	1.409	1.406
B10–C11	1.551	1.540	B10–C11	1.548	1.541
C11–C12	1.413	1.428	C11–C12	1.411	1.428
C11–C18	1.413	1.415	C11–C18	1.409	1.406
C12–O13	1.358	1.373	C12–O13	1.357	1.358
C12–C21	1.401	1.392	C12–C21	1.401	1.397
C14–C15	1.385	1.398	C14–C15	1.383	1.392
C15–C16	1.401	1.397	C15–C16	1.410	1.408
C16–C17	1.386	1.396	C16–C17	1.393	1.409
C18–C19	1.386	1.396	C16–C22	1.480	1.472
C19–C20	1.401	1.397	C18–C19	1.393	1.409
C20–C21	1.385	1.398	C19–C20	1.410	1.408
			C19–C28	1.480	1.472
			C20–C21	1.383	1.392
			C22–C23	1.404	1.408
			C22–C27	1.404	1.409
			C23–C24	1.393	1.391
			C24–C25	1.395	1.396
			C25–C26	1.395	1.396
			C26–C27	1.393	1.391
			C28–C29	1.404	1.409
			C28–C33	1.404	1.408
			C29–C30	1.393	1.391
			C30–C31	1.395	1.396
			C31–C32	1.395	1.396
			C32–C33	1.393	1.391

Table S2. Calculated bond lengths (Å) at S_0 and S_1 states for **2c** and **2d**.

2c	S_0	S_1	**2d**	S_0	S_1
C1–C2	1.394	1.416	C1–C2	1.405	1.437
C1–C6	1.405	1.392	C1–C6	1.405	1.394
C1–O13	1.350	1.336	C1–O13	1.347	1.328
C2–C3	1.395	1.394	C2–C3	1.400	1.400
C3–C4	1.395	1.394	C2–C22	1.481	1.465
C4–C5	1.394	1.416	C3–C4	1.400	1.400
C5–C6	1.405	1.392	C4–C5	1.405	1.437
C5–O7	1.350	1.336	C4–C28	1.481	1.465
C6–B10	1.522	1.538	C5–C6	1.405	1.394
O7–C8	1.358	1.370	C5–O7	1.347	1.328
C8–C9	1.412	1.430	C6–B10	1.526	1.543
C8–C14	1.398	1.388	O7–C8	1.356	1.380
C9–B10	1.548	1.535	C8–C9	1.411	1.421
C9–C17	1.412	1.416	C8–C14	1.401	1.389
B10–C11	1.548	1.535	C9–B10	1.550	1.539
C11–C12	1.412	1.430	C9–C17	1.413	1.417
C11–C18	1.412	1.416	B10–C11	1.550	1.539
C12–O13	1.358	1.370	C11–C12	1.411	1.421
C12–C21	1.398	1.388	C11–C18	1.413	1.417
C14–C15	1.393	1.406	C12–O13	1.356	1.380
C15–C16	1.410	1.414	C12–C21	1.401	1.389
C15–C22	1.480	1.469	C14–C15	1.385	1.399
C16–C17	1.383	1.387	C15–C16	1.402	1.396
C18–C19	1.383	1.387	C16–C17	1.386	1.394
C19–C20	1.410	1.414	C18–C19	1.386	1.394
C20–C21	1.393	1.406	C19–C20	1.402	1.396
C20–C28	1.480	1.469	C20–C21	1.385	1.399
C22–C23	1.404	1.409	C22–C23	1.403	1.409
C22–C27	1.404	1.409	C22–C27	1.404	1.410
C23–C24	1.393	1.391	C23–C24	1.393	1.389
C24–C25	1.395	1.396	C24–C25	1.394	1.396
C25–C26	1.395	1.396	C25–C26	1.395	1.396
C26–C27	1.392	1.391	C26–C27	1.393	1.390
C28–C29	1.404	1.409	C28–C29	1.403	1.409
C28–C33	1.404	1.409	C28–C33	1.404	1.410
C29–C30	1.393	1.391	C29–C30	1.393	1.389
C30–C31	1.395	1.396	C30–C31	1.394	1.396
C31–C32	1.395	1.396	C31–C32	1.395	1.396
C32–C33	1.392	1.391	C32–C33	1.393	1.390

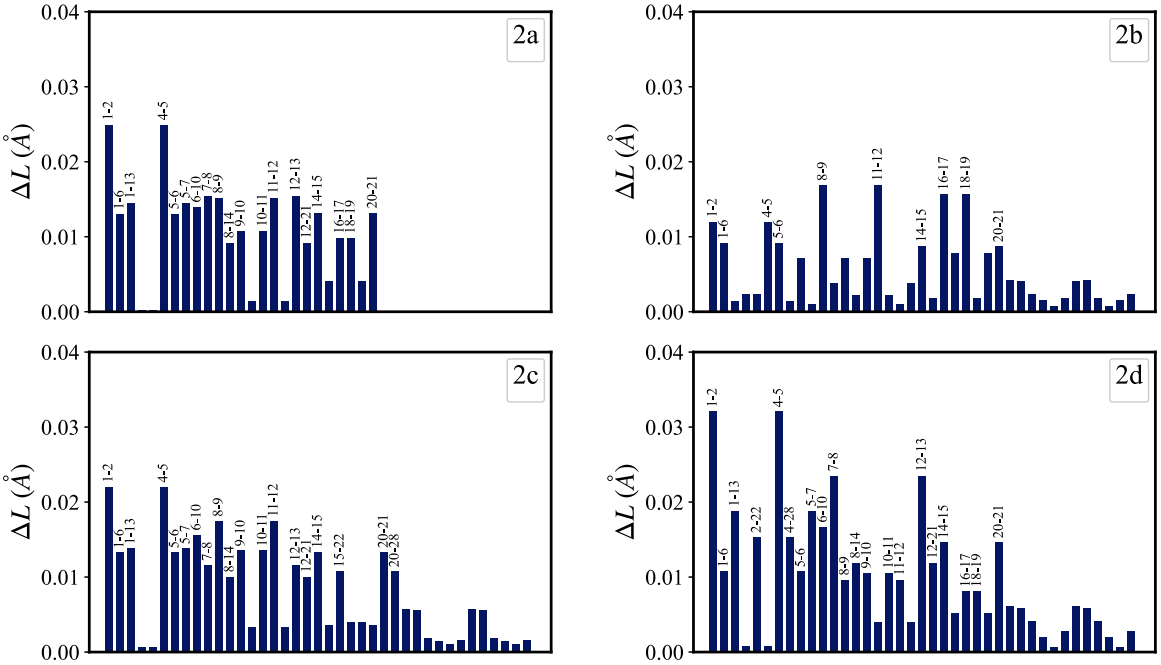

Figure S6. The absolute bond length difference between S_1 and S_0 states.

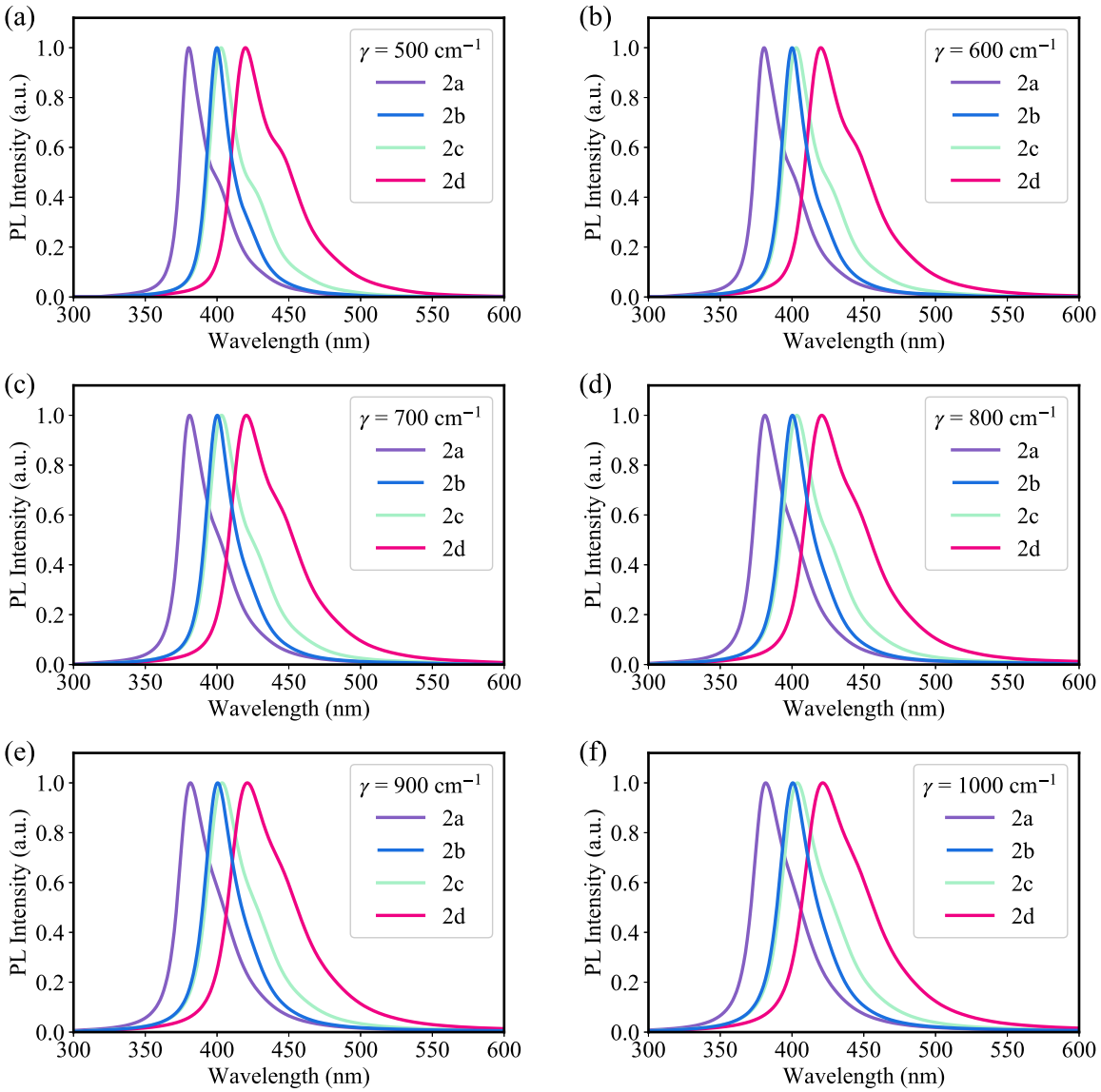

Figure S7. Calculated fluorescence emission spectra with different Lorentzian broadening values.

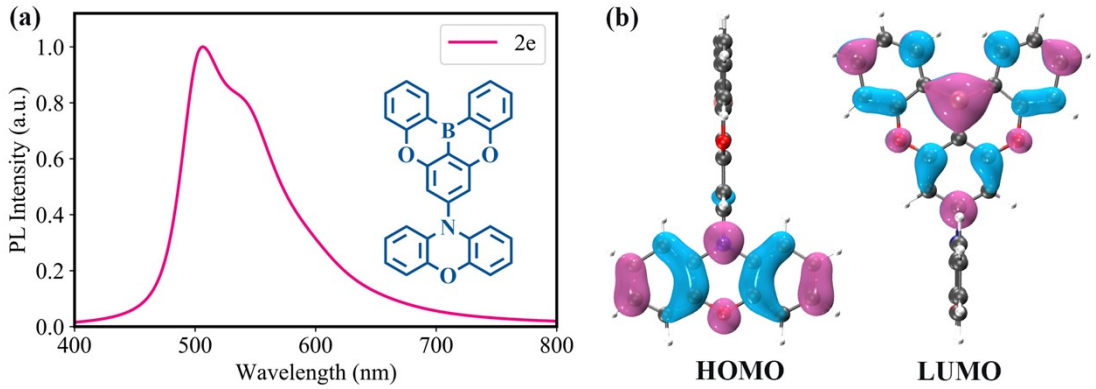

Figure S8. (a) Calculated fluorescence emission spectrum of **2e**. Here, the geometry optimizations and vibrational frequency calculations were performed at the CAM-B3LYP-D3BJ/def2-SVP level. (b) HOMO and LUMO distribution of **2e**.

Table S3. The BOBL parameters of studied compounds.

	η	2ϕ	κ
2a	0.062	−0.027	0.035
2b	0.054	−0.022	0.032
2c	0.059	−0.020	0.039
2d	0.063	−0.023	0.040
2e	0.096	0.000	0.096

As shown in **Table S3**, **2e** present the largest κ, which indicates a broad emission spectrum. The strong η can be attributed to localized HOMO and LUMO. Meantime, 2ϕ in **2e** is close to zero because of the spatial separation of HOMO and LUMO. Here, positive ϕ indicates the bonding character of HOMO and LUMO are different, one is localized bonding character and the other is antibonding character. Negative ϕ corresponds to the HOMO and LUMO with same bonding character.

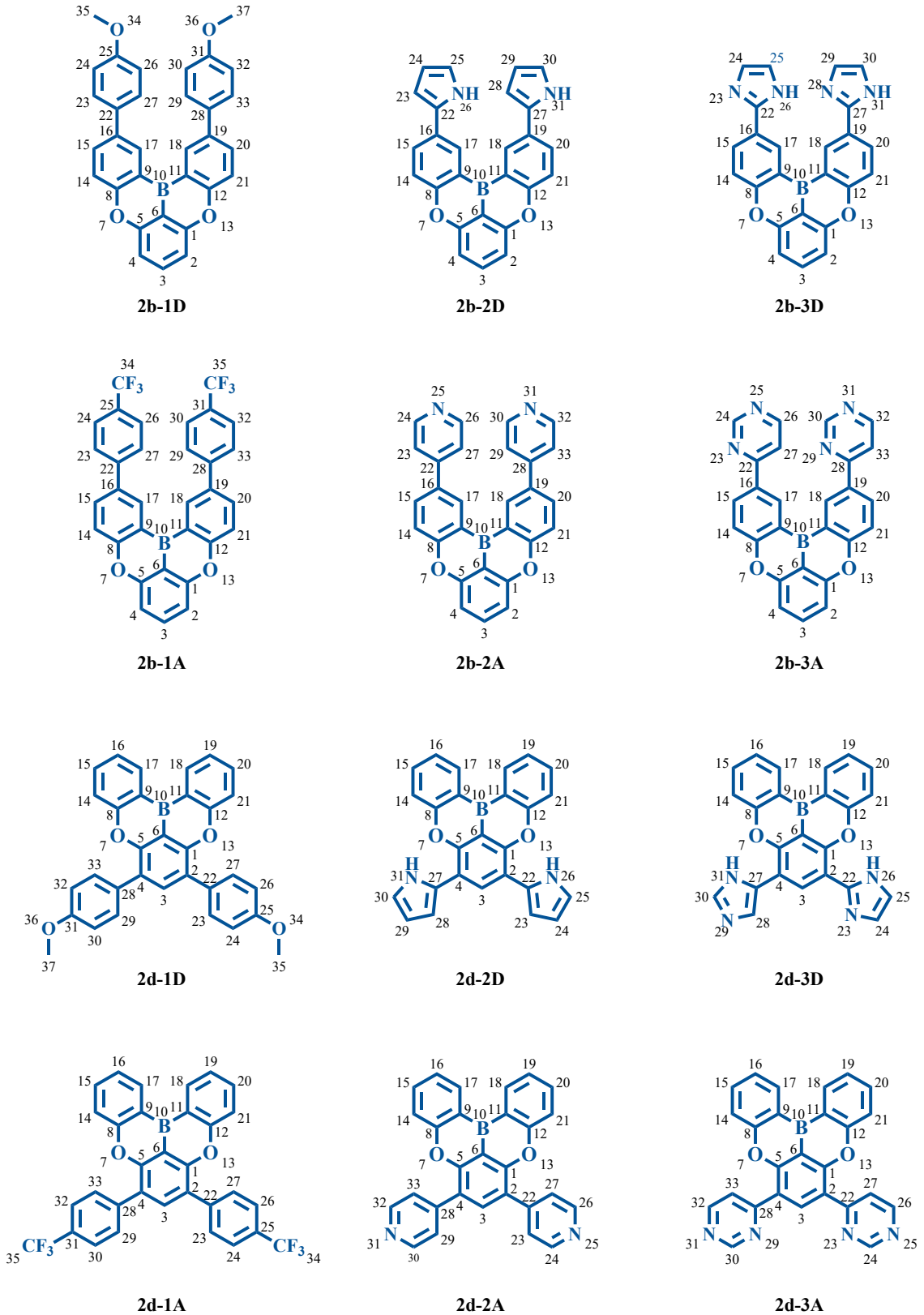

Figure S9. Chemical structures with atom index of **2b-** series and **2d-** series with different electron-donating and electron-withdrawing substituents.

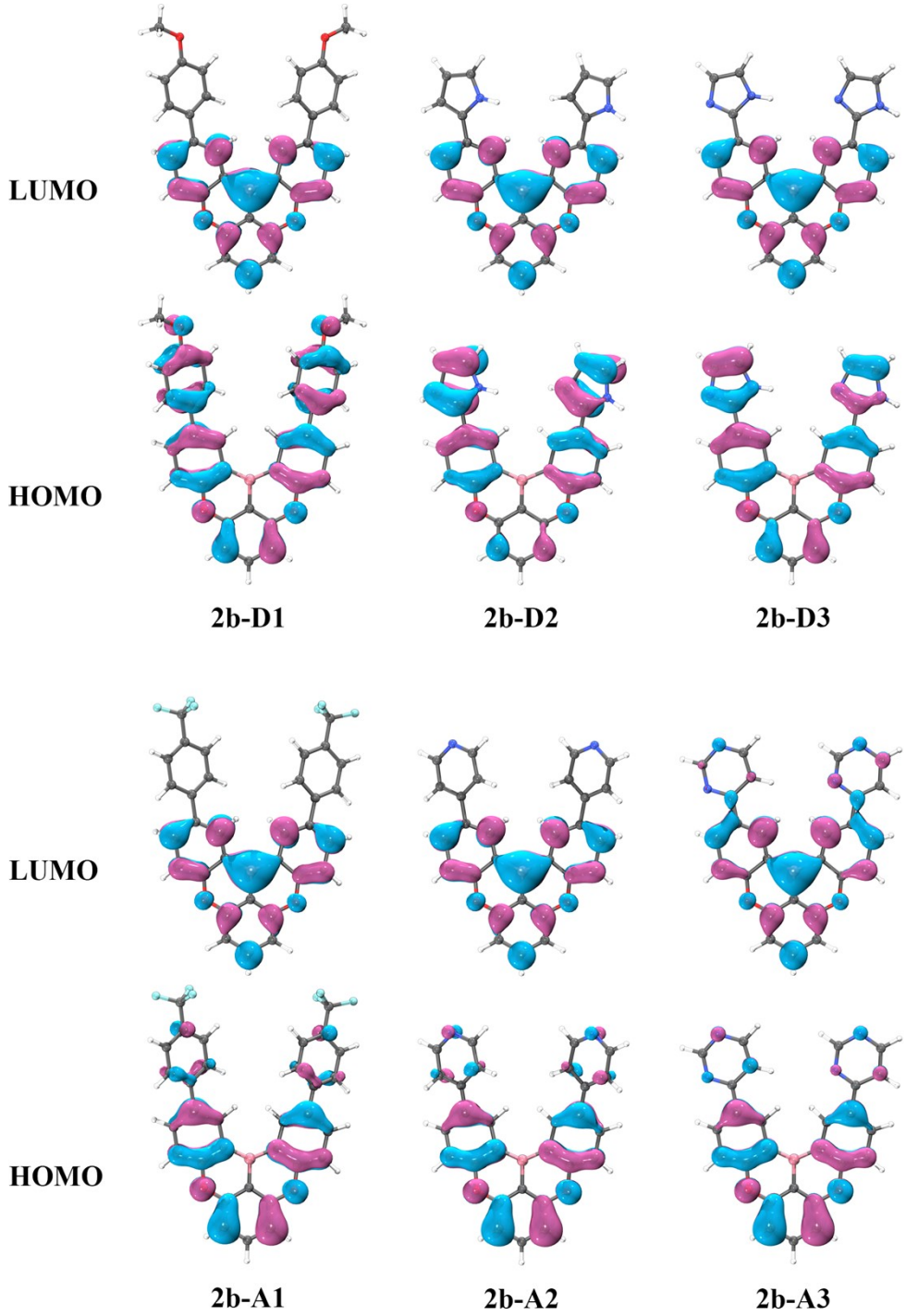

Figure S10. HOMO and LUMO distribution of **2b-D** series and **2b-A** series.

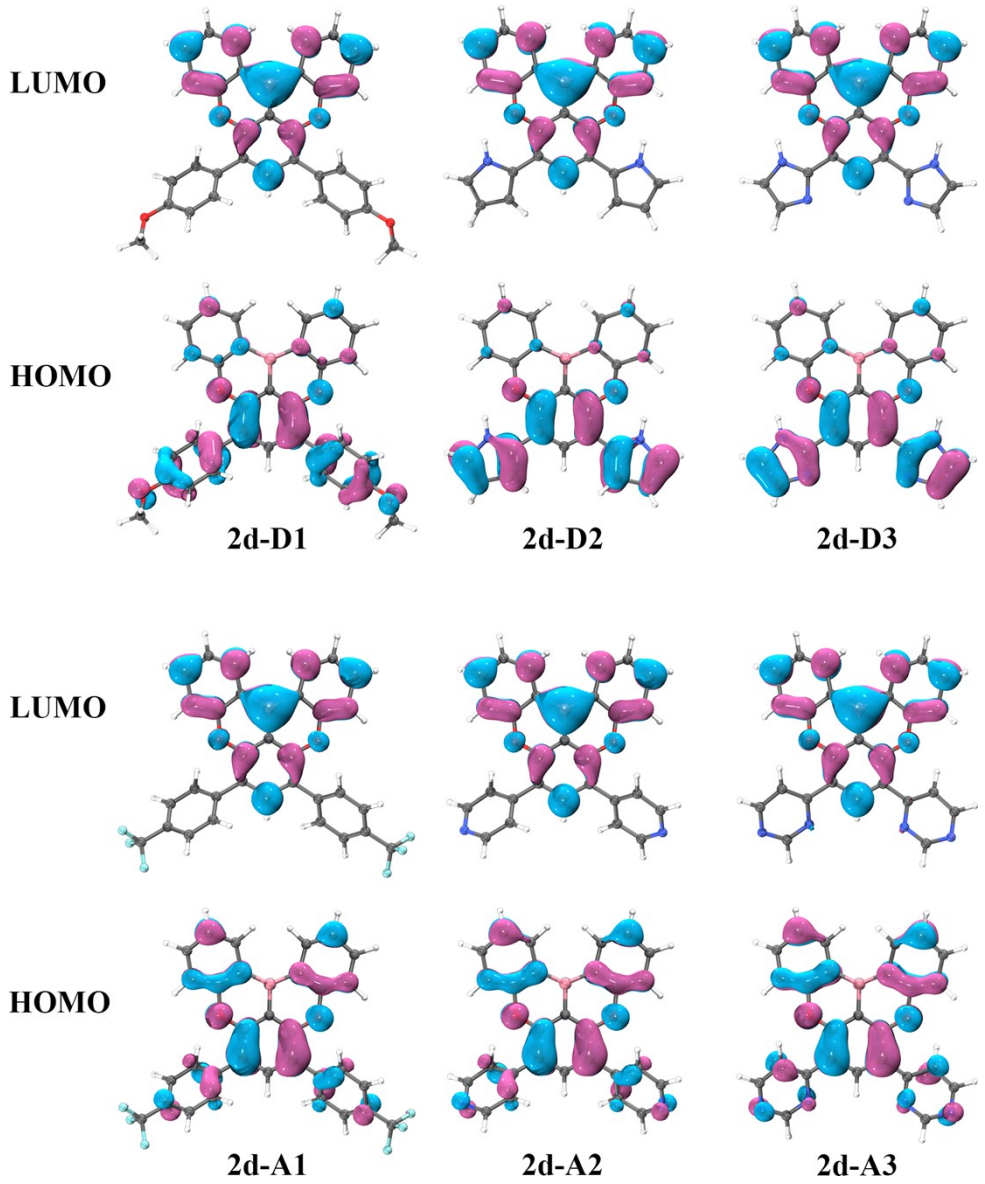

Figure S11. HOMO and LUMO distribution of **2d-D** series and **2d-A** series.

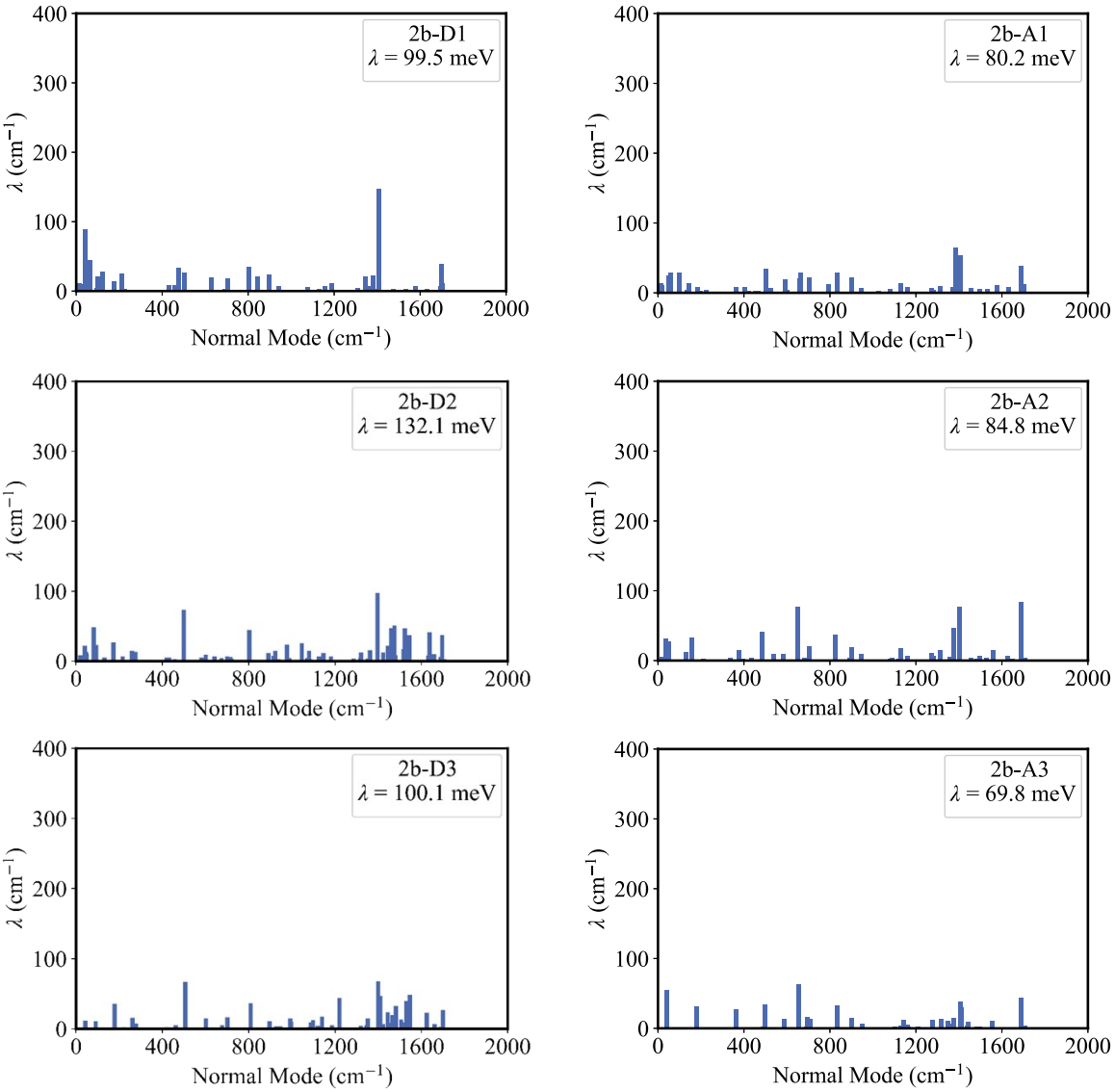

Figure 12. The contribution of the normal modes to the reorganization energy, for **2b-D** series and **2b-A** series.

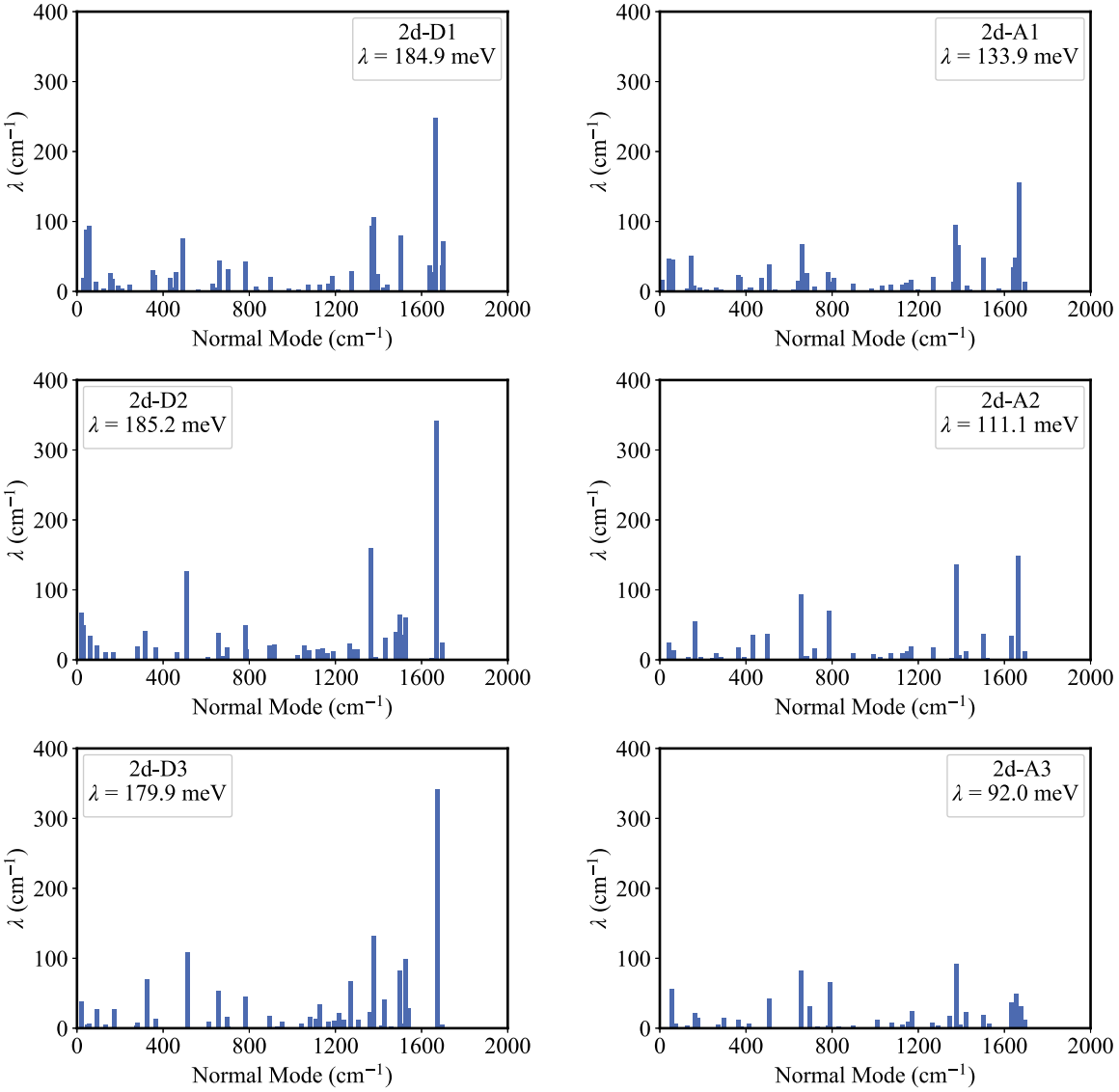

Figure S13. The contribution of the normal modes to the reorganization energy, for **2d-D** series and **2d-A** series.

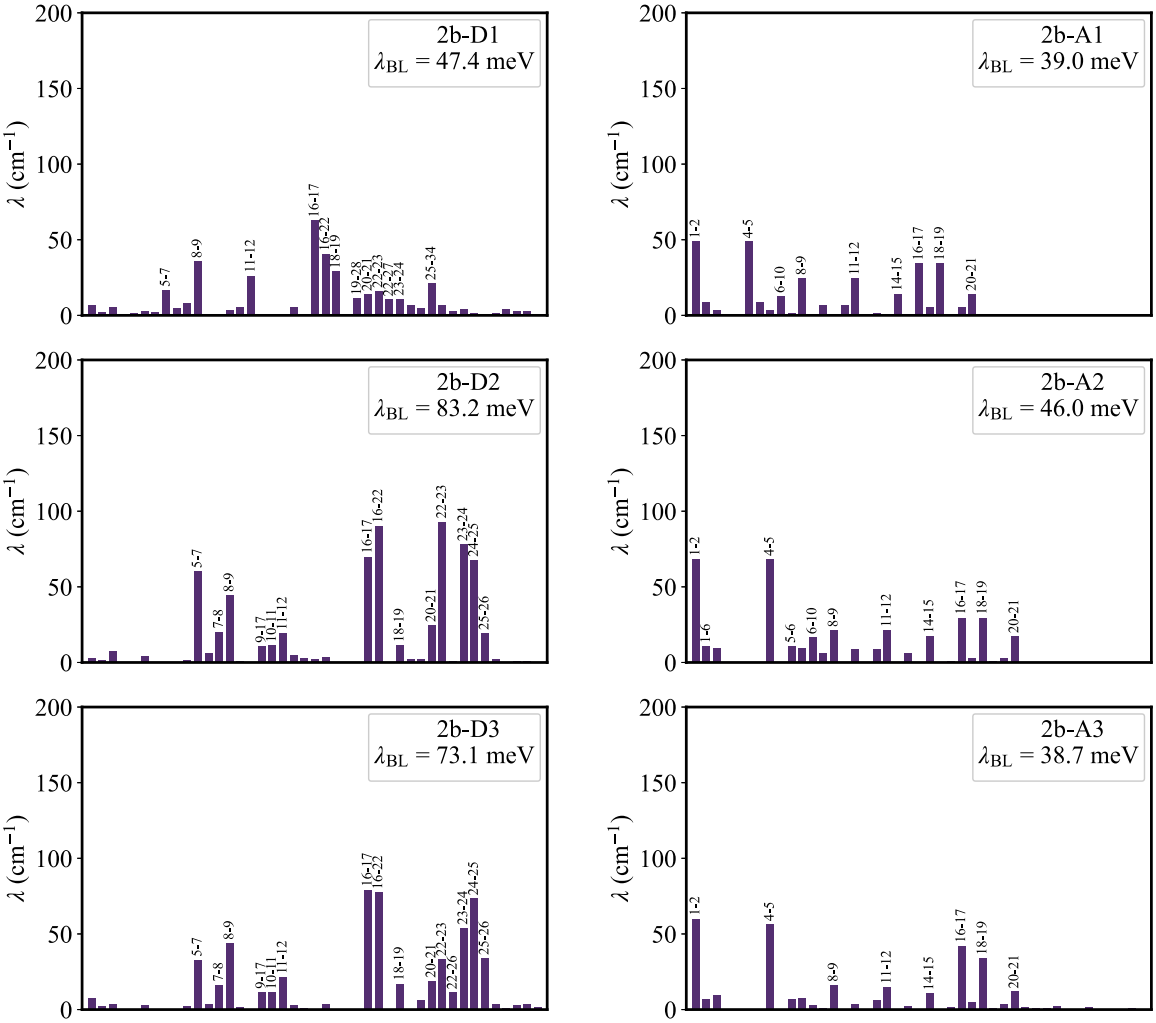

Figure S14. The contribution of chemical bonds to λ_{BL}, for **2b-D** series and **2b-A** series.

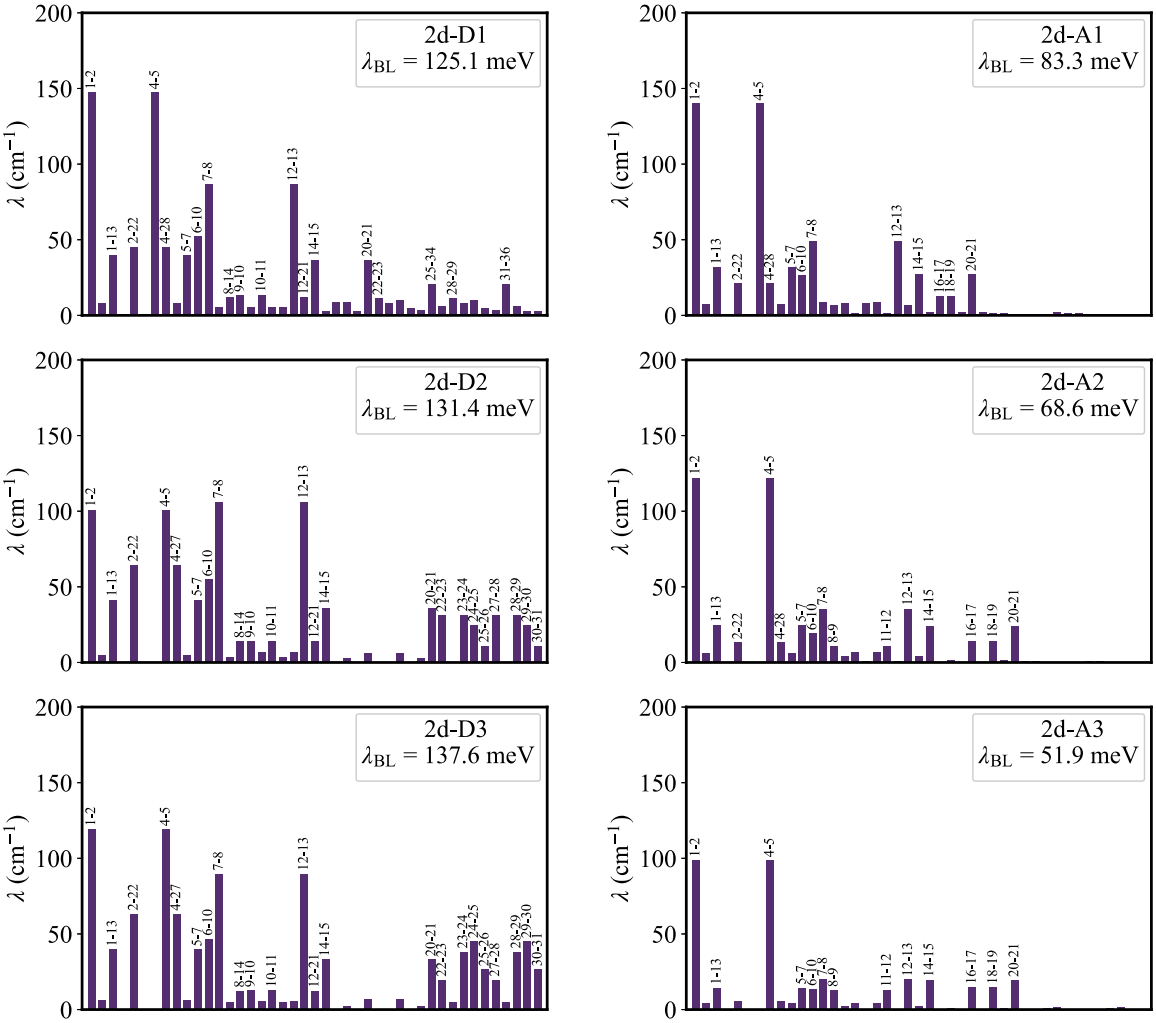

Figure S15. The contribution of chemical bonds to λ_{BL}, for **2d-D** series and **2d-A** series.

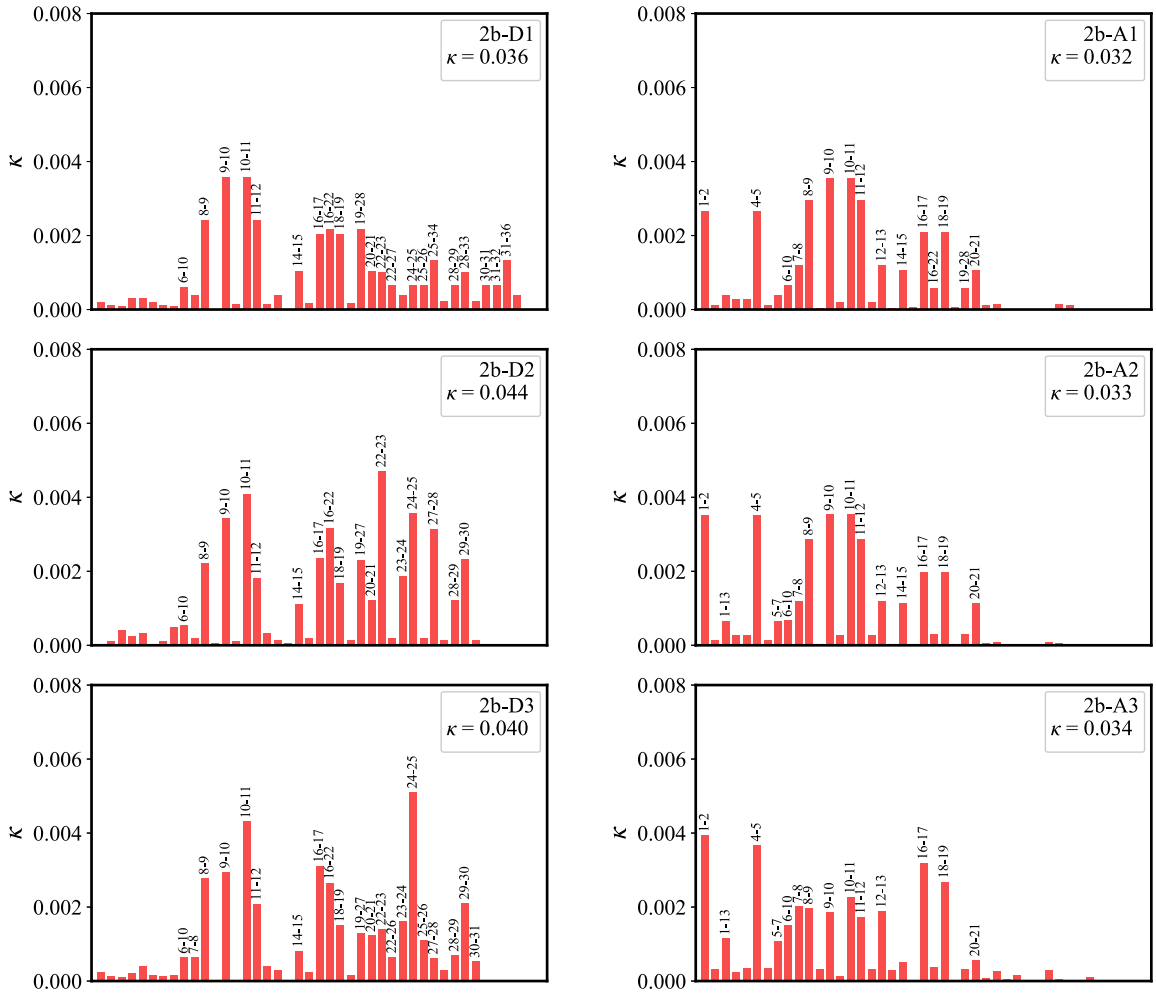

Figure S16. The contribution of chemical bonds to κ, for **2b-D** series and **2b-A** series.

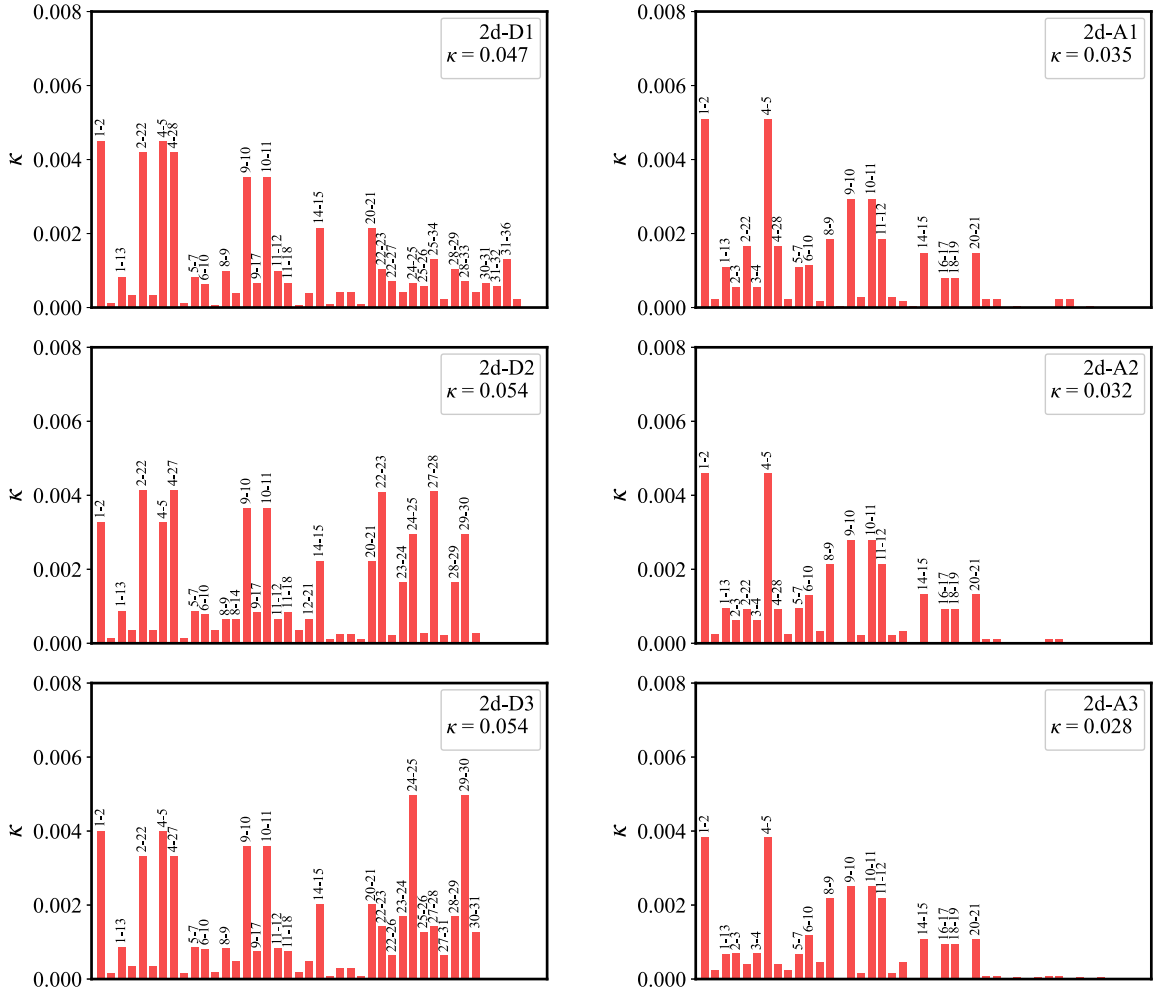

Figure S17. The contribution of chemical bonds to κ, for **2d-D** series and **2d-A** series.

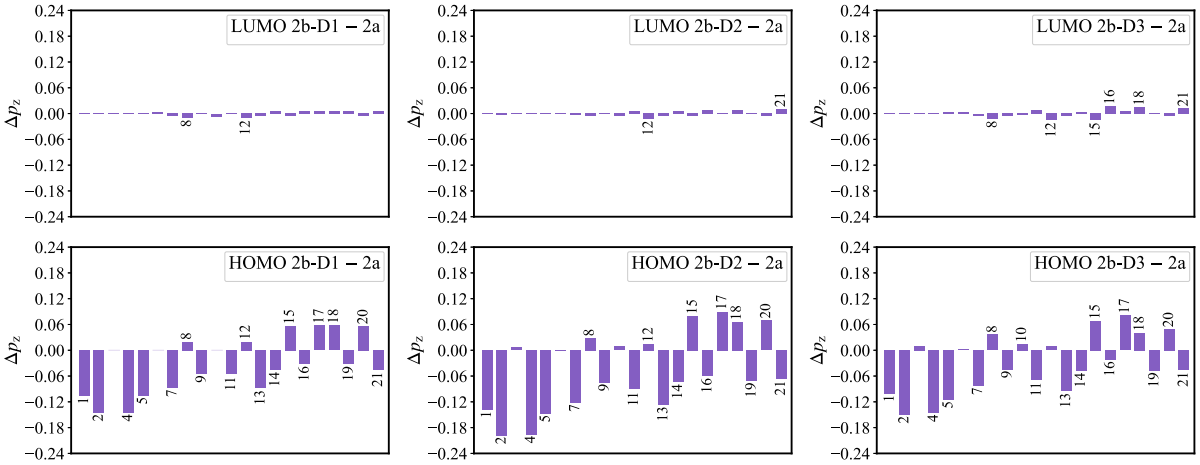

Figure S18. The variation of $p_{z(\textbf{2b-D}\ \text{series} - \textbf{2a})}$ on atoms.

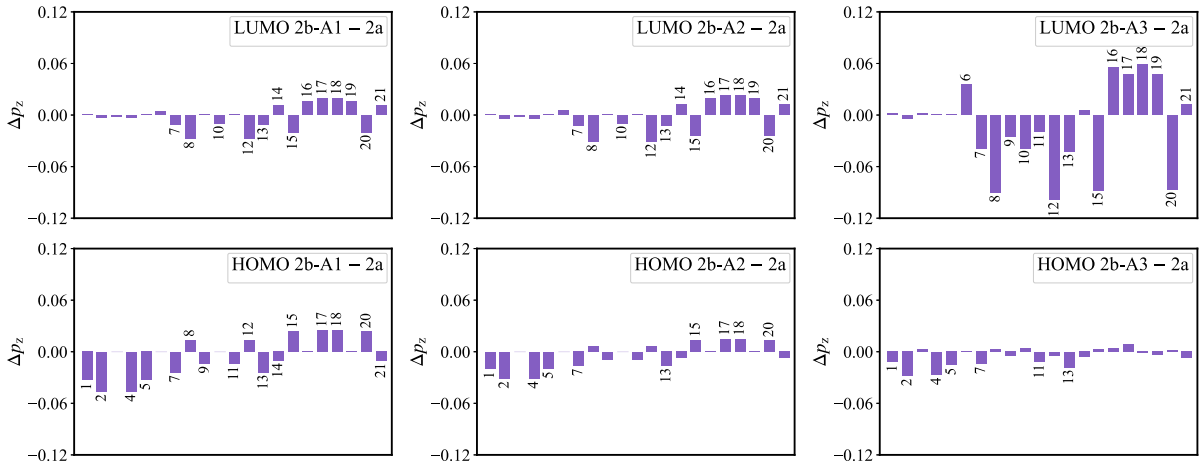

Figure S19. The variation of $p_{z(\textbf{2b-A}\text{ series} - \textbf{2a})}$ on atoms.

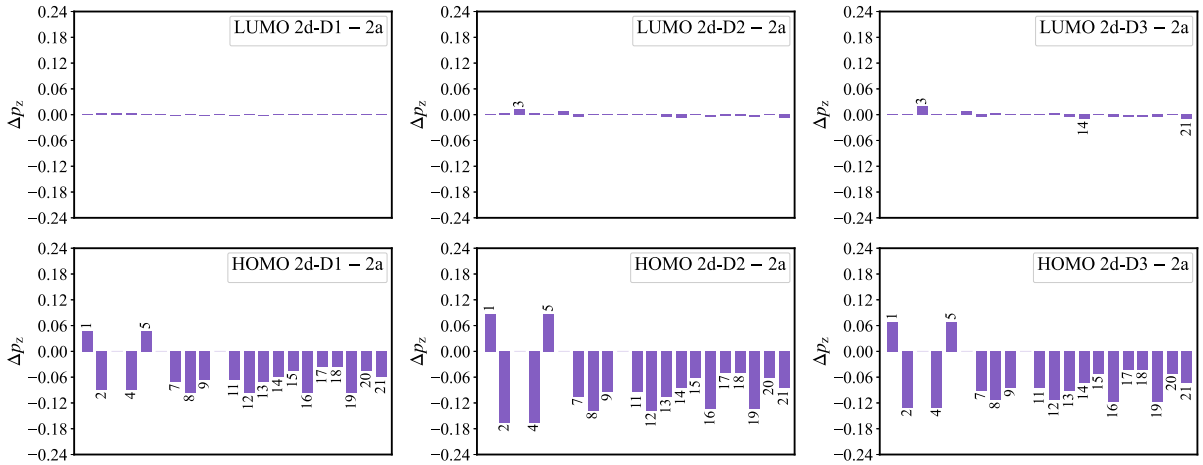

Figure S20. The variation of $p_{z(\textbf{2d-D}\text{ series} - \textbf{2a})}$ on atoms.

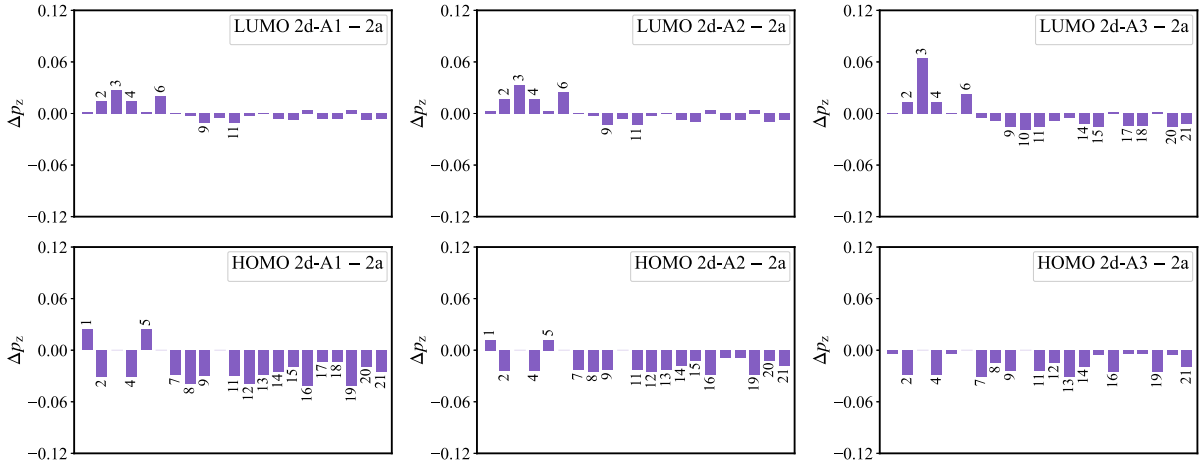

Figure S21. The variation of $p_{z(\textbf{2d-A}\text{ series} - \textbf{2a})}$ on atoms.

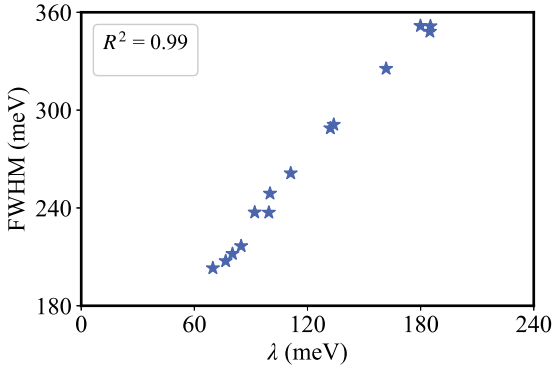

Figure S22. The correlation between reorganization energy and FWHM, for **2b**, **2b-D** series, **2b-A** series, **2d**, **2d-D** series, and **2d-A** series.